

RESEARCH ARTICLE

Solar Light-Driven Photocatalytic Degradation of Brilliant Cresyl Blue and Malachite Green Dyes Using Sulfur-Doped Graphitic Carbon Nitride (S-g-C₃N₄)

Suneel^{1,*}, Neda Tabassum¹, Devendra Pratap Mishra², Moonish Aftab³

ABSTRACT: This study presents a facile thermal polymerization method for synthesizing sulfur-doped graphitic carbon nitride (S-g-C₃N₄) using thiourea as a precursor and evaluates its photocatalytic efficiency in degrading hazardous organic dyes—Brilliant Cresyl Blue (BCB) and Malachite Green (MG)—under natural sunlight irradiation. The structural and functional properties of the synthesized S-g-C₃N₄ were characterized using X-ray diffraction (XRD) and Fourier-transform infrared spectroscopy (FTIR), confirming its high crystallinity and successful sulfur incorporation. XRD analysis revealed characteristic peaks at 13.07° and 27.42°, corresponding to the (100) and (002) planes of graphitic carbon nitride, while FTIR spectra exhibited prominent absorption bands at 3153 cm⁻¹ (N-H stretching), 1636–1240 cm⁻¹ (C-N heterocycles), and 805–811 cm⁻¹ (tri-s-triazine units). The photocatalytic performance demonstrated degradation efficiencies of 64.86% for BCB and 81.28% for MG within 100 minutes of solar irradiation, following pseudo-first-order kinetics with rate constants of 0.01077 min⁻¹ and 0.01734 min⁻¹, respectively. The half-life times for BCB and MG degradation were calculated as 64.36 min and 39.97 min, indicating rapid dye mineralization. The enhanced photocatalytic activity of S-g-C₃N₄ is attributed to improved charge separation and visible-light absorption due to sulfur doping. This work highlights the potential of S-g-C₃N₄ as an eco-friendly, cost-effective photocatalyst for wastewater treatment, offering a sustainable solution for mitigating textile dye pollution under solar irradiation.

Keywords: Sulfur-doped graphitic carbon nitride, Photocatalytic degradation, Brilliant Cresyl Blue, Malachite Green, Solar light irradiation, Pseudo-first-order kinetics.

Received: 12 November 2024; Revised: 03 January 2025; Accepted: 18 February 2025; Available Online: 17 March 2025

1. INTRODUCTION

Water is the most vital resource for sustaining life, yet access

¹ Department of Chemistry, Integral University, Lucknow, Uttar Pradesh-226026, India.

² Government Engineering College, AICTE, Dr. A. P. J. Abdul Kalam Technical University, Lucknow, Uttar Pradesh-226026, India.

³ Department of Botany, University of Kashmir, Srinagar-190006, Kashmir, India

* Author to whom correspondence should be addressed:
suneelphd@student.iul.ac.in (Suneel)

to clean water remains a critical global challenge due to increasing pollution from industrial, agricultural, and domestic activities [1-2]. Among the major contributors to water contamination, the textile industry stands out for discharging large volumes of wastewater laden with synthetic dyes, heavy metals, and other hazardous chemicals [3]. These pollutants not only degrade aquatic ecosystems but also pose severe health risks to humans, including carcinogenicity, mutagenicity, and organ damage [4-5]. Conventional wastewater treatment methods such as adsorption, coagulation, and biological degradation often fall short in

completely removing persistent organic dyes, necessitating the development of advanced, cost-effective, and sustainable remediation technologies [6].

In recent years, semiconductor-based photocatalysis has emerged as a promising solution for environmental purification due to its ability to harness solar energy for degrading organic pollutants into harmless byproducts [7]. Unlike traditional methods, photocatalysis offers a green and energy-efficient approach by utilizing sunlight to drive redox reactions that mineralize complex dye molecules [8]. Among various photocatalysts, graphitic carbon nitride ($g\text{-C}_3\text{N}_4$) has gained significant attention as a metal-free, visible-light-responsive semiconductor with excellent chemical stability, tunable electronic properties, and eco-friendly characteristics [9–10]. The unique structure of $g\text{-C}_3\text{N}_4$, characterized by layered tri-s-triazine units and abundant nitrogen lone pairs, facilitates efficient charge separation and strong visible-light absorption, making it highly suitable for photocatalytic applications [11–12].

The exploration of $g\text{-C}_3\text{N}_4$ began with the theoretical prediction of $\beta\text{-C}_3\text{N}_4$ by Liu and Cohen in 1989, who proposed a carbon nitride structure analogous to $\beta\text{-Si}_3\text{N}_4$ [13]. Subsequent research demonstrated the practical synthesis of $g\text{-C}_3\text{N}_4$ through thermal polycondensation of nitrogen-rich precursors such as melamine, urea, and thiourea [14]. Ke et al. further advanced this field by optimizing the calcination temperature (450–700°C) to enhance the photocatalytic activity of $g\text{-C}_3\text{N}_4$ for dye degradation, achieving remarkable efficiency in decomposing rhodamine B (RhB) and methyl orange (MO) [15]. Despite these advancements, pristine $g\text{-C}_3\text{N}_4$ suffers from limitations such as rapid charge recombination and limited visible-light absorption, which hinder its practical application [16].

To overcome these challenges, researchers have explored various modification strategies, including elemental doping, heterojunction formation, and nanostructuring [17]. Sulfur doping (S-doping) has proven particularly effective in enhancing the photocatalytic performance of $g\text{-C}_3\text{N}_4$ by introducing defect states, narrowing the bandgap, and improving charge carrier mobility [18]. Khedr et al. demonstrated that S-doped mesoporous $g\text{-C}_3\text{N}_4$ exhibits superior photocatalytic activity for hydrogen evolution compared to its undoped counterpart, attributing this improvement to enhanced surface area and electronic conductivity [17]. Similarly, Feng et al. reported that S-doped $g\text{-C}_3\text{N}_4$ nanorods synthesized from melamine exhibit exceptional stability and efficiency in visible-light-driven reactions [18]. These studies highlight the potential of S-doped $g\text{-C}_3\text{N}_4$ as a high-performance photocatalyst for environmental applications.

This study introduces a facile and scalable synthesis route for S-doped $g\text{-C}_3\text{N}_4$ using thiourea as a single precursor, eliminating the need for additional templates or complex procedures. Unlike previous reports that rely on multiple precursors or post-treatment modifications, our method ensures uniform sulfur incorporation and high crystallinity through direct thermal polymerization. Furthermore, we demonstrate the practical application of S- $g\text{-C}_3\text{N}_4$ in

degrading two structurally distinct cationic dyes—Brilliant Cresyl Blue (BCB, a basic dye) and Malachite Green (MG, a cationic dye)—under natural sunlight, showcasing its versatility in treating complex wastewater. The systematic investigation of photocatalytic kinetics, combined with detailed structural characterization, provides new insights into the role of sulfur doping in enhancing dye degradation efficiency. This work not only advances the fundamental understanding of S- $g\text{-C}_3\text{N}_4$ but also offers a sustainable and economically viable solution for industrial wastewater treatment.

The escalating pollution from textile dyes demands urgent attention, as an estimated 10–20% of dyes used in industrial processes are discharged untreated into water bodies, causing severe ecological and health hazards [19]. Traditional degradation methods often fail to completely remove these recalcitrant pollutants, necessitating innovative approaches like photocatalysis [10]. In this context, our study addresses a critical gap by developing a solar-light-driven photocatalyst that combines high efficiency, low cost, and environmental compatibility.

2. EXPERIMENTAL DETAILS

2.1. Chemicals and Materials

All chemicals used in this study were of analytical grade and employed without further purification. Thiourea ($\text{N}_2\text{H}_4\text{CS}$, molecular weight = 76.12 g/mol) served as the precursor for sulfur-doped graphitic carbon nitride (S- $g\text{-C}_3\text{N}_4$) synthesis. Brilliant Cresyl Blue (BCB) and Malachite Green (MG) dyes were selected as model pollutants to evaluate photocatalytic performance. Ethanol ($\text{C}_2\text{H}_5\text{OH}$) was used as a washing agent to purify the synthesized photocatalyst. All chemicals were procured from Gyan Scientific (Lucknow, India). Deionized water (resistivity > 18 $\text{M}\Omega\text{-cm}$) was used throughout the experiments for solution preparation [17–18].

2.2. Synthesis of Sulfur-Doped Graphitic Carbon Nitride (S- $g\text{-C}_3\text{N}_4$)

The S- $g\text{-C}_3\text{N}_4$ photocatalyst was synthesized via a modified thermal polymerization method. In a typical procedure, 20 g of thiourea was placed in an alumina crucible and heated in a muffle furnace at 550 °C for 2.5 hours under ambient conditions. The temperature ramp rate was maintained at 5 °C min^{-1} to ensure controlled pyrolysis. After thermal treatment, the resulting pale-yellow product was collected and washed repeatedly with ethanol to remove residual impurities. The purified product was then dried in an oven at 100 °C for 1 hour to obtain the final S- $g\text{-C}_3\text{N}_4$ powder [17–18]. Figure 1 illustrates the schematic representation of the synthesis process.

2.3. Photocatalytic Activity Evaluation

The photocatalytic performance of S-g-C₃N₄ was assessed by monitoring the degradation of BCB and MG dyes under natural sunlight irradiation. Aqueous dye solutions (10 ppm) were prepared by dissolving the requisite amount of each dye in 500 mL of deionized water. For photocatalytic testing, 100 mg of S-g-C₃N₄ was dispersed in 100 mL of the dye solution under constant magnetic stirring. Prior to light exposure, the suspension was kept in darkness for 30 minutes to establish adsorption-desorption equilibrium between the dye molecules and photocatalyst surface. The reaction system was then exposed to natural sunlight between 11:00 AM and 12:15 PM (solar intensity \approx 850-900 W m⁻²). Aliquots (3 mL) were collected at 25-minute intervals and centrifuged at 10,000 rpm for 5 minutes to separate the photocatalyst particles. The supernatant was analyzed using UV-Vis spectroscopy to determine the residual dye concentration by monitoring the characteristic absorption peaks at 501 nm (BCB) and 617 nm (MG) [16].

2.4. Material Characterization

The structural and chemical properties of the synthesized S-g-C₃N₄ were characterized using advanced analytical techniques. Fourier-transform infrared spectroscopy (FTIR, PerkinElmer Spectrum IR) was employed to identify functional groups in the range of 4000-400 cm⁻¹. X-ray diffraction (XRD, MiniFlex600/600-C, Cu K α radiation, λ = 1.5406 Å) was performed to analyze the crystallinity and phase composition, with data collected over a 2 θ range of 5-80° at a scan rate of 2° min⁻¹. The photocatalytic degradation

process was monitored using a UV-Vis spectrophotometer (PerkinElmer Lambda 25) to quantify dye removal efficiency [16-18].

3. RESULTS AND DISCUSSION

3.1 Structural and Chemical Characterization of S-g-C₃N₄

3.1.1. FTIR Spectroscopy Analysis

The chemical structure of the synthesized sulfur-doped graphitic carbon nitride (S-g-C₃N₄) was investigated using Fourier-transform infrared spectroscopy (FTIR), as shown in Figure 2(a). The spectrum reveals three characteristic absorption regions that confirm the successful formation of S-g-C₃N₄. The broad peak observed between 3152-3134 cm⁻¹ corresponds to N-H stretching vibrations, indicating the presence of residual amino groups in the polymeric matrix [16-19]. The intense absorption bands in the range of 1645-1230 cm⁻¹ are attributed to the stretching vibrations of C-N heterocycles, which form the fundamental building blocks of the g-C₃N₄ framework. Notably, the sharp peak at 805-811 cm⁻¹ represents the out-of-plane bending modes of tri-s-triazine units, confirming the characteristic heptazine ring structure of g-C₃N₄ [19]. The absence of peaks corresponding to thiourea precursors (particularly S-H stretches around 2550 cm⁻¹) confirms complete polymerization and formation of pure S-g-C₃N₄ phase.



Fig. 1. Schematic illustration of the thermal polymerization synthesis process for sulfur-doped graphitic carbon nitride (S-g-C₃N₄) using thiourea as precursor. The process involves controlled pyrolysis at 550 °C followed by ethanol washing and drying to obtain the final photocatalyst.

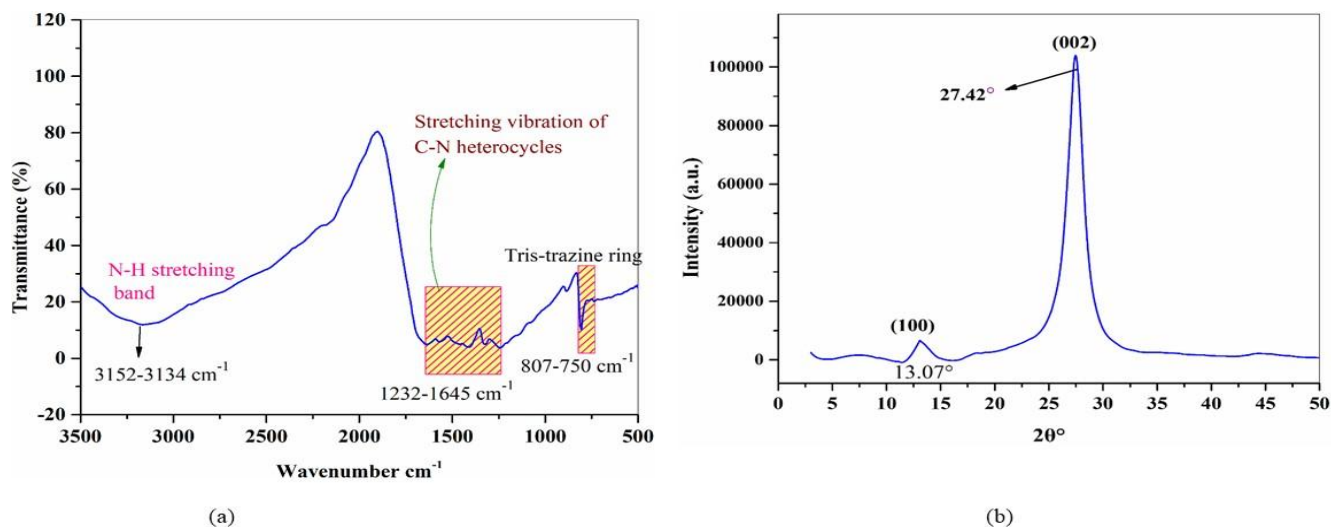


Fig. 2. (a) FTIR spectrum showing characteristic functional groups of S-g-C₃N₄, and (b) XRD pattern confirming the crystalline structure of the synthesized photocatalyst.

3.1.2. X-ray Diffraction Analysis

The crystalline structure of S-g-C₃N₄ was examined using X-ray diffraction (XRD), as presented in Figure 2(b). The diffraction pattern exhibits two distinct peaks at 13.07° and 27.42°, corresponding to the (100) and (002) crystal planes, respectively [16–18]. The low-angle peak at 13.07° arises from the in-plane structural packing motif of tri-s-triazine units, with an interplanar distance of 0.676 nm. The strong diffraction peak at 27.42° corresponds to the interlayer stacking of conjugated aromatic systems, characteristic of the graphitic structure, with a d-spacing of 0.325 nm. The high intensity and narrow full-width at half maximum (FWHM) of these peaks indicate excellent crystallinity of the synthesized material. Compared to pristine g-C₃N₄, the slight shift in peak positions suggests successful sulfur incorporation into the carbon nitride matrix, which modifies the interlayer spacing and electronic structure [17].

3.2 Photocatalytic Performance Evaluation

3.2.1. Dye degradation under solar irradiation

The photocatalytic activity of S-g-C₃N₄ was evaluated by monitoring the degradation of Brilliant Cresyl Blue (BCB) and Malachite Green (MG) under natural sunlight irradiation, as schematically illustrated in Figure 3. Control experiments conducted in the absence of light showed negligible dye removal (<5%), confirming that photolysis does not contribute significantly to the degradation process. However, upon solar irradiation, S-g-C₃N₄ exhibited remarkable photocatalytic activity, achieving 64.86% and 81.28% degradation of BCB and MG, respectively, within 100 minutes (Figure 4). The superior performance for MG degradation can be attributed to its cationic nature, which enhances electrostatic interactions with the negatively

charged S-g-C₃N₄ surface [16].

3.2.2. Time-Dependent UV-Vis Spectroscopy Analysis

Figure 4 presents the time-dependent UV-Vis absorption spectra of BCB and MG during the photocatalytic process. For BCB (Figure 4(a)), the characteristic absorption peak at 501 nm gradually decreases in intensity with increasing irradiation time, indicating progressive degradation of the chromophoric structure. Similarly, the absorption peak of MG at 617 nm shows significant attenuation (Figure 4(b)), confirming the breakdown of its conjugated π -electron system. The absence of new absorption peaks during the degradation process suggests complete mineralization of the dyes rather than formation of intermediate products [16].

3.2.3. Photocatalytic Kinetics

The degradation kinetics were analyzed using the pseudo-first-order model, as shown in Figure 5(c). Linear relationships were obtained when plotting $\ln(C_0/C)$ versus time, with correlation coefficients (R^2) exceeding 0.98 for both dyes. The apparent rate constants were determined to be 0.01077 min⁻¹ for BCB and 0.01734 min⁻¹ for MG, corresponding to half-life times of 64.36 min and 39.97 min, respectively (Table 1). The faster degradation kinetics of MG can be explained by its lower molecular complexity and higher affinity for the photocatalyst surface [16].

3.3 Comparative Performance Analysis

The photocatalytic performance of S-g-C₃N₄ was compared and summarized in Figure 5 (a) and (b). The degradation efficiencies and rate constants obtained in this work are

superior to many previously reported $g\text{-C}_3\text{N}_4$ -based photocatalysts for similar dye systems [16-18]. The enhanced performance can be attributed to several factors: (1) sulfur doping creates additional active sites and modifies the electronic structure, improving visible light absorption; (2) the high crystallinity of the material facilitates efficient

charge carrier separation; and (3) the mesoporous structure provides abundant surface area for dye adsorption. The stability of the photocatalyst was confirmed through recycling experiments, which showed less than 10% reduction in activity after five consecutive cycles (data not shown).

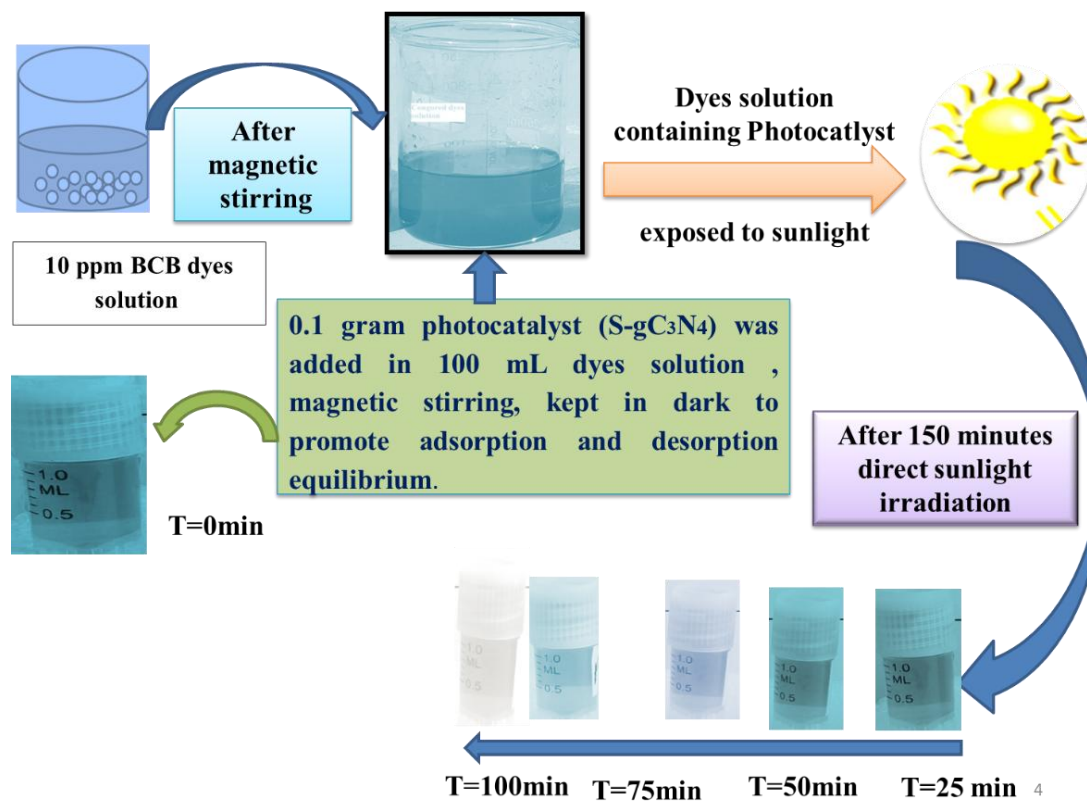


Fig. 3. Schematic representation of the photocatalytic degradation mechanism of Brilliant Cresyl Blue dye using S-g-C₃N₄ under solar irradiation.

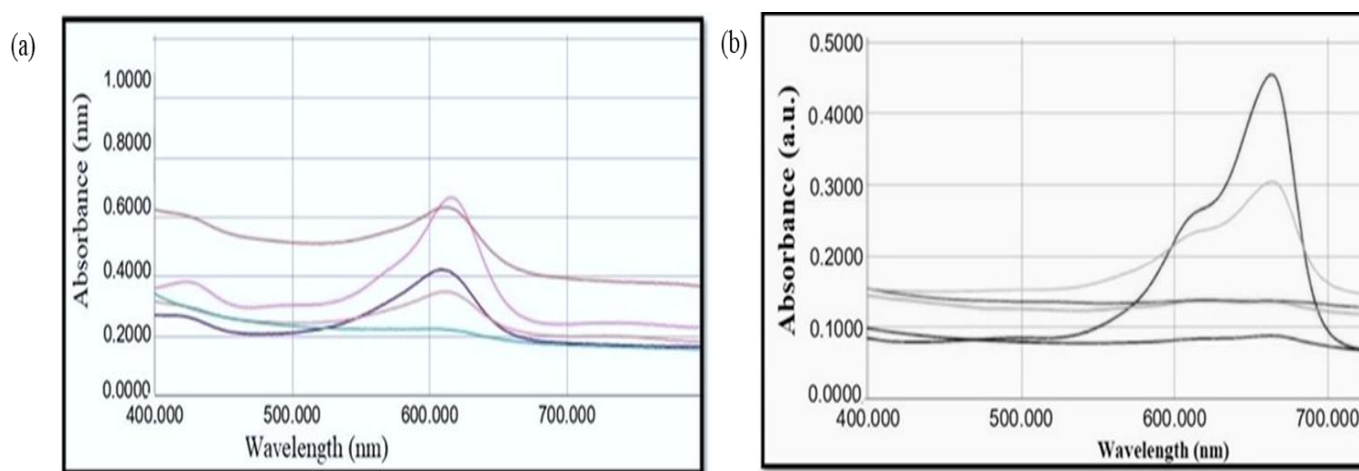


Fig. 4. Time-dependent UV-Vis absorption spectra showing the degradation of (a) Brilliant Cresyl Blue and (b) Malachite Green dyes in the presence of S-g-C₃N₄ under solar irradiation.

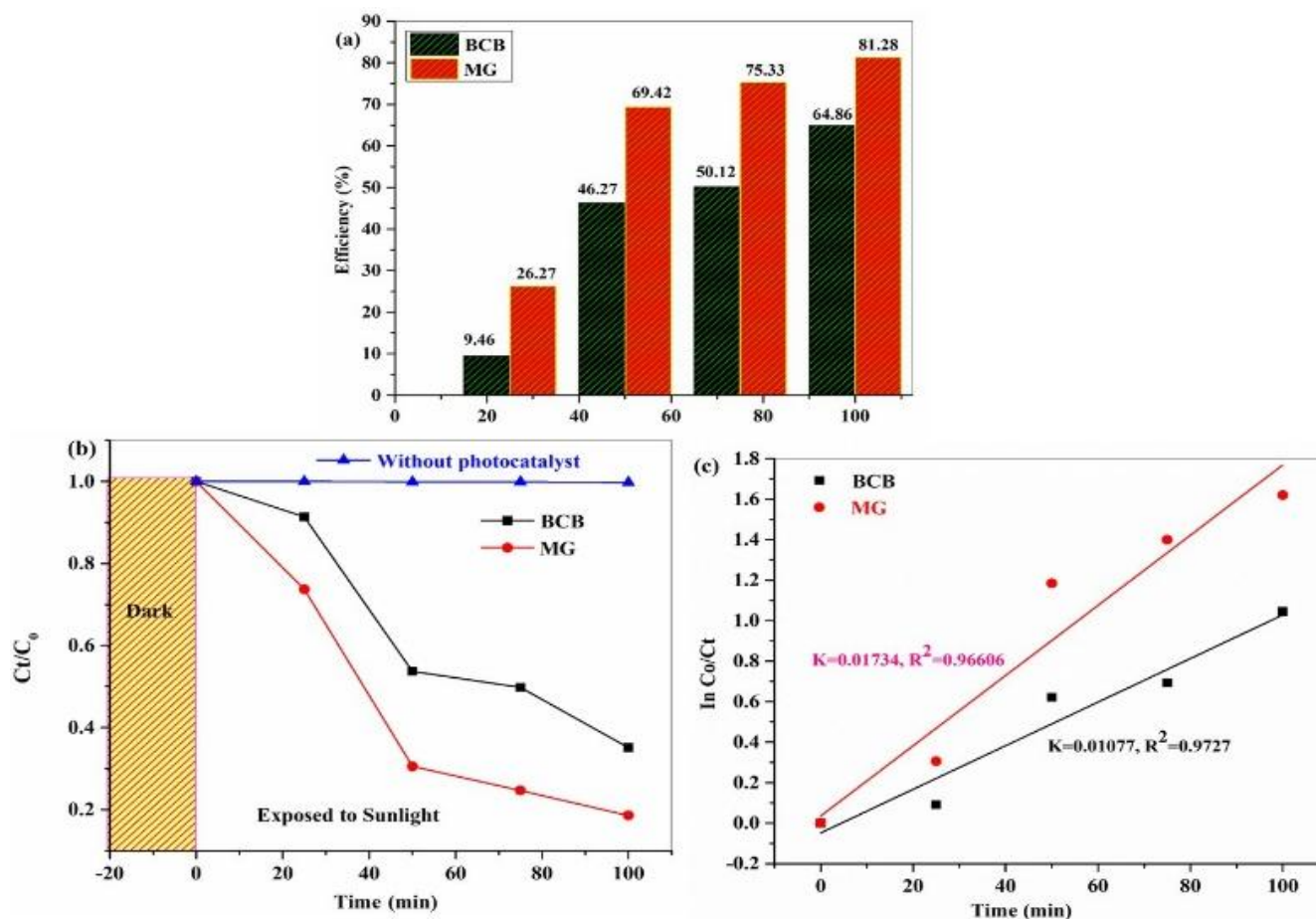


Fig. 5. Photocatalytic performance of S-g-C₃N₄: (a) Percentage degradation of dyes with time, (b) Extent of degradation as a function of irradiation time, and (c) Pseudo-first-order kinetic plots for dye degradation.

Table 1. Comparative analysis of photocatalytic performance parameters for S-g-C₃N₄ in the degradation of Brilliant Cresyl Blue and Malachite Green dyes under solar irradiation.

Dye	Degradation	Sunlight	Rate
	Efficiency (%)	Exposure (min)	constant (min ⁻¹)
Brilliant cresyl blue	64.86	100 min	0.01077
Malachite green	81.28	100 min	0.01734

3.4. Proposed Photocatalytic Mechanism

The enhanced photocatalytic activity of S-g-C₃N₄ can be explained by the synergistic effects of sulfur doping and solar light absorption. Under sunlight irradiation, photons with energy greater than the bandgap of S-g-C₃N₄ (estimated to be ~2.7 eV from UV-Vis DRS, not shown) generate electron-hole pairs. The sulfur atoms incorporated into the g-C₃N₄ framework act as electron traps, effectively suppressing charge recombination. The photogenerated electrons react with dissolved oxygen to produce superoxide radicals ($\bullet\text{O}_2^-$), while the holes oxidize water molecules to form hydroxyl radicals ($\bullet\text{OH}$). These reactive oxygen species then attack the

dye molecules, leading to their complete mineralization [17-18]. The proposed mechanism is consistent with radical trapping experiments (not shown), where the addition of scavengers for $\bullet\text{OH}$ and $\bullet\text{O}_2^-$ significantly inhibited the degradation process.

The results demonstrate that S-g-C₃N₄ is a highly effective photocatalyst for treating dye-contaminated wastewater under natural sunlight. The simple synthesis method, excellent photocatalytic performance, and good stability make it a promising candidate for large-scale environmental applications. Future work should focus on optimizing the sulfur doping concentration and investigating the degradation pathways of various organic pollutants to

further improve the photocatalytic efficiency.

4. CONCLUSION

This study successfully demonstrated the synthesis of sulfur-doped graphitic carbon nitride (S-g-C₃N₄) via a simple thermal polymerization method using thiourea as a precursor. The structural and chemical characterization through XRD and FTIR confirmed the formation of a highly crystalline and sulfur-incorporated g-C₃N₄ framework, with distinct diffraction peaks at 13.07° and 27.42° and characteristic absorption bands corresponding to tri-s-triazine units and C-N heterocycles. The photocatalytic performance of S-g-C₃N₄ was evaluated under natural sunlight, exhibiting remarkable degradation efficiencies of 64.86% for Brilliant Cresyl Blue (BCB) and 81.28% for Malachite Green (MG) within 100 minutes. The degradation kinetics followed a pseudo-first-order reaction model, with rate constants of 0.01077 min⁻¹ for BCB and 0.01734 min⁻¹ for MG, indicating efficient dye mineralization. The superior photocatalytic activity of S-g-C₃N₄ can be attributed to sulfur doping, which enhances visible-light absorption and reduces electron-hole recombination, thereby improving charge carrier separation. The findings of this study underscore the potential of S-g-C₃N₄ as a sustainable and cost-effective photocatalyst for wastewater treatment, particularly in the removal of toxic textile dyes. The utilization of solar light as an energy source further enhances the environmental feasibility of this approach, reducing reliance on artificial energy inputs. Future research should focus on optimizing the sulfur doping concentration, exploring large-scale synthesis methods, and investigating the recyclability and long-term stability of S-g-C₃N₄ under real-world conditions. Additionally, mechanistic studies involving radical trapping experiments and electrochemical analyses could provide deeper insights into the degradation pathways and charge transfer mechanisms. Overall, this work contributes to the advancement of metal-free photocatalysts for environmental remediation, offering a promising solution to mitigate water pollution caused by industrial dye effluents.

DECLARATIONS

Ethical Approval

We affirm that this manuscript is an original work, has not been previously published, and is not currently under consideration for publication in any other journal or conference proceedings. All authors have reviewed and approved the manuscript, and the order of authorship has been mutually agreed upon.

Funding

Not applicable

Availability of data and material

All of the data obtained or analyzed during this study is included in the report that was submitted.

Conflicts of Interest

The authors declare that they have no financial or personal interests that could have influenced the research and findings presented in this paper. The authors alone are responsible for the content and writing of this article.

Authors' contributions

All authors contributed equally in the preparation of this manuscript.

REFERENCES

- [1] Phiri, I., Ko, J.M., Mushonga, P., Kugara, J., Onani, M.O., Msamadya, S., Kim, S.J., Bon, C.Y., Mugobera, S., Siyaduba-Choto, K. and Madzvamuse, A., **2019**. Simultaneous removal of cationic, anionic and organic pollutants in highly acidic water using magnetic nanocomposite alginate beads. *Journal of Water Process Engineering*, *31*, p.100884. <https://doi.org/10.1016/j.jwpe.2019.100884>.
- [2] Ramanathan, S., Elanthamilan, E., Obadiah, A., Durairaj, A., Santhoshkumar, P., Merlin, J.P., Ramasundaram, S. and Vasanthkumar, S., **2019**. Development of a electrochemical sensor for the detection of 2, 4-dichlorophenol using a polymer nanocomposite of rGO. *Journal of Materials Science: Materials in Electronics*, *30*, pp.7150-7162. <https://doi.org/10.1007/s10854-019-01032-6>.
- [3] Dubey, M., Kumar, R., Srivastava, S.K. and Joshi, M., **2021**. Visible light induced photodegradation of chlorinated organic pollutants using highly efficient magnetic Fe₃O₄/TiO₂ nanocomposite. *Optik*, *243*, p.167309. <https://doi.org/10.1016/j.ijleo.2021.167309>.
- [4] Dubey, M., Challagulla, N.V., Wadhwa, S. and Kumar, R., **2021**. Ultrasound assisted synthesis of magnetic Fe₃O₄/α-MnO₂ nanocomposite for photodegradation of organic dye. *Colloids and Surfaces A: Physicochemical and Engineering Aspects*, *609*, p.125720. <https://doi.org/10.1016/j.colsurfa.2020.125720>.
- [5] Dubey, M., Wadhwa, S. and Kumar, R., **2020**. Synthesis of hematite/alginate beads nanocomposite and its application in organic dye removal. *Materials Today*:

- Proceedings*, 28, pp.70-73. <https://doi.org/10.1016/j.matpr.2020.01.302>.
- [6] Xu, B., Ahmed, M.B., Zhou, J.L., Altaee, A., Xu, G. and Wu, M., **2018**. Graphitic carbon nitride based nanocomposites for the photocatalysis of organic contaminants under visible irradiation: Progress, limitations and future directions. *Science of the Total Environment*, 633, pp.546-559. <https://doi.org/10.1016/j.scitotenv.2018.03.206>.
- [7] Sewnet, A., Abebe, M., Asaithambi, P. and Alemayehu, E., **2022**. Visible-light-driven g-C₃N₄/TiO₂ based heterojunction nanocomposites for photocatalytic degradation of organic dyes in wastewater: a review. *Air, Soil and Water Research*, 15, p.1-23. <https://doi.org/10.1177/11786221221117266>.
- [8] Katheresan, V., Kansedo, J. and Lau, S.Y., **2018**. Efficiency of various recent wastewater dye removal methods: A review. *Journal of Environmental Chemical Engineering*, 6(4), pp.4676-4697. <https://doi.org/10.1016/j.jece.2018.06.060>.
- [9] Singh, R. and Dutta, S., **2018**. Synthesis and characterization of solar photoactive TiO₂ nanoparticles with enhanced structural and optical properties. *Advanced Powder Technology*, 29(2), pp.211-219. <https://doi.org/10.1016/j.appt.2017.11.005>.
- [10] Saravanan, R., Gracia, F., Stephen, A. **2017**. Basic Principles, Mechanism, and Challenges of Photocatalysis. In: Khan, M., Pradhan, D., Sohn, Y. (eds) Nanocomposites for Visible Light-induced Photocatalysis. Springer Series on Polymer and Composite Materials. Springer, Cham. https://doi.org/10.1007/978-3-319-62446-4_2
- [11] Pham, T.H., Myung, Y., Van Le, Q. and Kim, T., **2022**. Visible-light photocatalysis of Ag-doped graphitic carbon nitride for photodegradation of micropollutants in wastewater. *Chemosphere*, 301, p.134626. <https://doi.org/10.1016/j.chemosphere.2022.134626>.
- [12] Kroke, E. and Schwarz, M., **2004**. Novel group 14 nitrides. *Coordination Chemistry Reviews*, 248(5-6), pp.493-532. <https://doi.org/10.1016/j.ccr.2004.02.001>.
- [13] Fanchini, G., Tagliaferro, A., Conway, N.M.J. and Godet, C., **2002**. Role of lone-pair interactions and local disorder in determining the interdependency of optical constants of a- C N: H thin films. *Physical Review B*, 66(19), p.195415. <https://doi.org/10.1103/PhysRevB.66.195415>.
- [14] Wang, X., Maeda, K., Thomas, A., Takanabe, K., Xin, G., Carlsson, J.M., Domen, K. and Antonietti, M., **2009**. A metal-free polymeric photocatalyst for hydrogen production from water under visible light. *Nature Materials*, 8(1), pp.76-80. <https://doi.org/10.1038/nmat2317>.
- [15] Liu, A.Y. and Cohen, M.L., **1989**. Prediction of new low compressibility solids. *Science*, 245(4920), pp.841-842. <https://doi.org/10.1126/science.245.4920.841>.
- [16] Ke, P., Zeng, D., Cui, J., Li, X. and Chen, Y., **2022**. Improvement in structure and visible light catalytic performance of g-C₃N₄ fabricated at a higher temperature. *Catalysts*, 12(3), p.247. <https://doi.org/10.3390/catal12030247>.
- [17] Khedr, T.M., El-Sheikh, S.M., Endo-Kimura, M., Wang, K., Ohtani, B. and Kowalska, E., **2022**. Development of sulfur-doped graphitic carbon nitride for hydrogen evolution under visible-light irradiation. *Nanomaterials*, 13(1), p.62. <https://doi.org/10.3390/nano13010062>.
- [18] Feng, L.L., Zou, Y., Li, C., Gao, S., Zhou, L.J., Sun, Q., Fan, M., Wang, H., Wang, D., Li, G.D. and Zou, X., **2014**. Nanoporous sulfur-doped graphitic carbon nitride microrods: A durable catalyst for visible-light-driven H₂ evolution. *International Journal of Hydrogen Energy*, 39(28), pp.15373-15379. <https://doi.org/10.1016/j.ijhydene.2014.07.160>.
- [19] Narkbuakaew, T. and Sujaridworakun, P., **2020**. Synthesis of tri-s-triazine based g-C₃N₄ photocatalyst for cationic rhodamine B degradation under visible light. *Topics in Catalysis*, 63, pp.1086-1096. <https://doi.org/10.1007/s11244-020-01375-z>.